

TEXTURE DEFECT DETECTION USING SUBBAND DOMAIN CO-OCCURRENCE MATRICES

Ahmet Latif Amer¹, Aysin Ertüzün¹, Aytül Erçil²

¹Department of Electrical-Electronics Engineering

²Department of Industrial Engineering

Bogaziçi University

Bebek 80815, Istanbul, TURKEY.

latif@busim.ee.boun.edu.tr, ertuz@boun.edu.tr, ercil@boun.edu.tr

ABSTRACT

In this paper, a new defect detection algorithm for textured images is presented. The algorithm is based on the subband decomposition of gray level images through wavelet filters and extraction of the co-occurrence features from the subband images. Detection of defects within the inspected texture is performed by partitioning the textured image into non-overlapping subwindows and classifying each subwindow as defective or non-defective with a mahalanobis distance classifier being trained on defect free samples a priori. The experimental results demonstrating the use of this algorithm for the visual inspection of textile products obtained from the real factory environment are also presented.

I. INTRODUCTION

Visual inspection constitutes an important part of quality control in industry. Until recent years, this job has been heavily relied upon human inspectors. Development of fast and specialized equipment, however, has facilitated the application of image processing algorithms to real world industrial inspection problems.

Texture analysis has nearly three decades long past. During the seventies and early eighties, the algorithms have been mainly based on first and second order statistics of the image pixel gray level values as spatial domain gray level co-occurrence matrix (SDCM) and neighboring gray level dependence matrix (NGLDM) [5,11,12]. In mid-eighties, model based methods as Markov Random Fields (MRF), simultaneous autoregressive (SAR) models and Gibbs distribution have appeared as an alternative. Starting from the late eighties, however, by the theoretical impact of the works of Daubechies [4], who has provided the discretization of the wavelet transform (WT), and Mallat [9], who has established the connection between the WT and the multiresolution theory, signal processing methods based on Gabor transform and the WT have replaced the former two [1,2,6]. Representing signals in multiple resolutions by the WT is believed to enable extraction of more powerful features than the single scale case. Features extracted are, mainly, based on band energy and

entropy. Although frequency based features work well for most applications, it can not be argued that this will be true for all of the cases as shown in [12] and [10], where statistical features outperformed the former. In this study, a new method, namely, the subband domain co-occurrence matrix (SBCM) method [7] is presented. It is shown how combined use of two approaches, i.e. extracting frequency based features through signal processing methods (such as WT) and statistical features from SDCM can lead to effective solutions for the texture analysis problems particularly, the texture defect detection. WT is used to determine the frequency bands carrying the most information about the texture by decomposing the images into multiple frequency bands and computing the band energies. This can be viewed as dimensionality reduction or removing the irrelevant data prior to the feature extraction process. Then Haralick features [5] are extracted from the co-occurrence matrices computed from the subbands that represent the texture best. In the detection part, mahalanobis distance classifier is used to decide whether the test image is defective or not.

Organization of the paper is as follows: Section II introduces the background theory for the co-occurrence matrices and the WT. Section III describes the proposed texture defect detection system. Implementation details and experimental results are summarized in Section IV. Finally, Section V includes the concluding remarks.

II. MATHEMATICAL FRAMEWORK

A. Co-occurrence Matrices

A co-occurrence matrix is a square matrix with elements corresponding to the relative frequency of occurrence of pairs of gray level of pixels separated by a certain distance in a given direction. Formally, the elements of a $G \times G$ gray level co-occurrence matrix $P_{\mathbf{d}}$ for a displacement vector $\mathbf{d} = (dx, dy)$ is defined as :

$$P_{\mathbf{d}}(i, j) = |\{(r, s), (t, v) : I(r, s) = i, I(t, v) = j\}| \quad (1)$$

where $I(\cdot, \cdot)$ denote an image of size $N \times N$ with G gray values, $(r, s), (t, v) \in N \times N$, $(t, v) = (r + dx, s + dy)$ and $|\cdot|$ is the cardinality of a set.

Haralick, Shanmugan and Dinstein [5] proposed 14 measures of textural features which are derived from the co-occurrence matrices, and each represents certain image properties as coarseness, contrast, homogeneity and texture complexity. Those that are used, in this work, for extracting features in the defect detection of textured images are:

1) *Entropy* :

$$\text{ENT} = -\sum_i \sum_j p(i, j) \log p(i, j) \quad (2)$$

Entropy gives a measure of complexity of the image. Complex textures tend to have higher entropy.

2) *Contrast* :

$$\text{CON} = \sum_i \sum_j (i - j)^2 p(i, j) \quad (3)$$

Contrast feature is a measure of the image contrast or the amount of local variations present in an image.

3) *Angular Second Moment* :

$$\text{ASM} = \sum_i \sum_j \{p(i, j)\}^2 \quad (4)$$

Angular second moment is a measure of the homogeneity of an image. Hence it is a suitable measure for detection of disorders in textures. For homogeneous textures value of angular second moment turns out to be small compared to non-homogeneous ones.

4) *Inverse Difference Moment* :

$$\text{IDM} = \sum_i \sum_j \frac{1}{1 + (i - j)^2} p(i, j) \quad (5)$$

In Eqs. (2) - (5), $p(i, j)$ refers to the normalized entry of the co-occurrence matrices. That is $p(i, j) = P_{\mathbf{d}}(i, j)/R$ where R is the total number of pixel pairs (i, j) . For a displacement vector $\mathbf{d} = (dx, dy)$ and image of size $N \times M$ R is given by $(N-dx)(M-dy)$.

B. Wavelet Transform

The WT is defined as a decomposition of a signal with a family of real orthonormal basis functions, $\mathbf{y}_{m,n}(x)$, obtained through translation and dilation of a kernel function $\mathbf{y}(x)$ known as the mother wavelet [4-9].

$$\mathbf{y}_{m,n}(x) = 2^{-m/2} \mathbf{y}(2^{-m}x - n) \quad (6)$$

where m and n are integers. Since $\mathbf{y}_{m,n}(x)$ form an orthonormal set, the analysis and synthesis formula for a signal $f(x)$ are, respectively, given by

$$c_{m,n} = \int_{-\infty}^{+\infty} f(x) \mathbf{y}_{m,n}(x) dx \quad (7)$$

$$f(x) = \sum_{m,n} c_{m,n} \mathbf{y}_{m,n}(x) \quad (8)$$

The mother wavelet can be constructed first determining a scaling function satisfying the two-scale difference equation

$$\mathbf{f}(x) = \sqrt{2} \sum_k h(k) \mathbf{f}(2x - k) \quad (9)$$

and then relating $\mathbf{y}(x)$ to the scaling function via

$$\mathbf{y}(x) = \sqrt{2} \sum_k g(k) \mathbf{f}(2x - k) \quad (10)$$

where

$$g(k) = (-1)^k h(1-k). \quad (11)$$

Nice thing about this decomposition scheme is that one does not need to calculate explicitly the scaling and mother wavelet functions, but can obtain the transform coefficients, recursively, using $h(k)$ and $g(k)$. A J -level decomposition can be written as

$$\begin{aligned} f(x) &= \sum_k c_{0,k} \mathbf{f}_{0,k}(x) \\ &= \sum_k (c_{J+1,k} \mathbf{f}_{J+1,k}(k) + \sum_{j=0}^J d_{j+1,k} \mathbf{y}_{j+1,k}(x)) \end{aligned} \quad (12)$$

where coefficients $c_{0,k}$ are given and coefficients $c_{j+1,n}$ and $d_{j+1,n}$ at scale $j+1$ are related to the coefficients $c_{j,n}$ at scale j via

$$c_{j+1,n} = \sum_k c_{j,k} h(k - 2n) \quad (13a)$$

$$d_{j+1,n} = \sum_k d_{j,k} g(k - 2n) \quad (13b)$$

for $0 \leq j \leq J$.

In signal processing terms, operations in Eq. (13) is nothing but convolving coefficients $c_{j,n}$ and $d_{j,n}$ at resolution j with $\tilde{h}(n)$ and $\tilde{g}(n)$ and downsampling by two (dropping every other sample) to obtain $c_{j+1,n}$ and $d_{j+1,n}$. Here $\tilde{h}(n)$ and $\tilde{g}(n)$ are defined as

$$\tilde{h}(n) = h(-n) \quad (14a)$$

$$\tilde{g}(n) = g(-n) \quad (14b)$$

and can be regarded as impulse responses of quadrature mirror lowpass and highpass filters H and G , respectively. The output of J -level decomposition will contain the low-resolution coefficient $c_{J,n}$ and detail coefficients $d_{j,n}$ for each level ($1 \leq j \leq J$) (Fig.1).

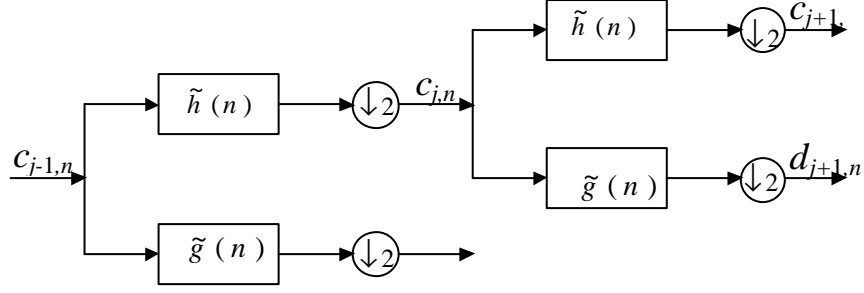


Fig. 1. Two-level wavelet decomposition scheme

III. TEXTURE DEFECT DETECTION

A. General Overview

Texture defect detection can be defined as the process of determining the location and/or the extend of a collection of pixels in a textured image with remarkable deviation in their intensity values or spatial arrangement with respect to the background texture.

Majority of texture defect detection applications are on textile, paper, steel and wood inspection. Most recent work on texture defect detection is that of Cohen *et al* [3] and Lee *et al* [8] with application to textile fabric and steel strip inspections, respectively. Cohen's method is based on modeling textile fabric images through MRF and use of easily computable sufficient statistics as features in place of model parameters during the classification of samples as defective or non-defective via a generalized likelihood test. The latter, have used neural networks to classify defects through energy and entropy features computed from the adaptive wavelet packet expansion of the steel images.

The proposed defect detection system consists of two stages [7]: (i) The feature extraction part which first utilizes the WT to decompose textured images into subbands and then extracts co-occurrence features from the subbands and (ii) the detection part which is a mahalanobis distance classifier being trained by defect-free samples. The algorithms for each are provided below:

B. Feature Extraction

Given an image $I(n,m)$ of size 256×256 , the following steps are applied to extract subband domain features:

i- Decompose image $I(n,m)$ into four bands using wavelet filter coefficients to obtain images I_{LL} , I_{LH} , I_{HL} and I_{HH} where L and H represent lowpass and highpass bands, respectively (Fig.2).

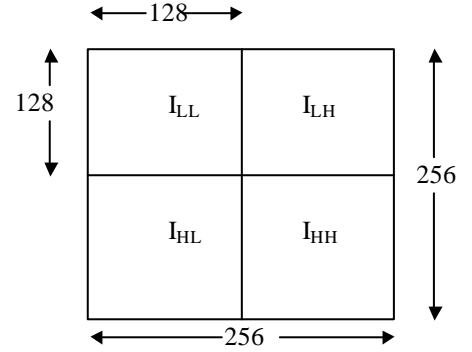


Fig. 2. Decomposition of Image $I(n,m)$

ii- Calculate energy e_x of each decomposed image as:

$$e_x = \frac{1}{N^2} \sum_n \sum_m |I_x(n,m)|$$

where $N = 128$ and x denotes LL, LH, HL and HH bands.

iii- If energy of a subband in the decomposed image is significantly lower than the maximum subband energy, discard this band and consider only the remaining subbands. That is, consider bands with $e_x > C e_{\max}$ where C is a constant less than one.

iv- Divide each subband image into non-overlapping subwindows $S_{x,i}$ of size 16×16 . Indices x and i denote subband and subwindows, respectively ($1 \leq i \leq 64$). Subwindow of this size corresponds to a subwindow S_i of size 32×32 in the original image.

v- Derive the co-occurrence matrices P_θ for $d=1$ (pixel separation distance) and angles $\mathbf{q} = (0, \pi/4, \pi/2, 3\pi/4)$ radians.

vi- Calculate ENT, CON, ASM, IDM for each co-occurrence matrix as in Eqs. (2)-(5).

vii- Compute mean \mathbf{m}_k and standard deviation \mathbf{s}_k for each feature of four angles.

viii- Construct the vector

$$\mathbf{f}_{x,i} = [\mathbf{m}_{ENT} \mathbf{s}_{ENT} \mathbf{m}_{CON} \mathbf{s}_{CON} \mathbf{m}_{ASM} \mathbf{s}_{ASM} \mathbf{m}_{DM} \mathbf{s}_{IDM}].$$

ix-Repeat steps (v) to (viii) for all bands (x) being retained according to the argument in step (iii).

x- Feature vector for i -th subwindow S_i in the original image is constructed as :

$$\mathbf{s}_i = [\mathbf{f}_{LL,i} \mathbf{f}_{LH,i} \dots]^T.$$

xi- Repeat steps (v) to (x) for all i .

C. Detection

The detection part of the system consists of a learning phase and a classification phase. These phases will be elaborated in the subsequent parts.

Learning phase

(i) Given k defect-free 256x256 fabric images, calculate the feature vectors for each subwindow of the image using the feature extraction scheme given above. Consider these vectors as the true feature vectors and name them as \mathbf{t}_i ($1 \leq i \leq 64k$).

(ii) Compute the mean vector \mathbf{m} and the covariance matrix \mathbf{C} for the feature vectors \mathbf{t}_i .

Classification phase

(i) Given a test image calculate the feature vectors \mathbf{s}_i 's using the feature extraction scheme given above.

(ii) Compute the mahalanobis distance d_i between each feature vector \mathbf{s}_i and the mean vector \mathbf{m}

$$d_i = (\mathbf{s}_i - \mathbf{m})^T \mathbf{C}^{-1} (\mathbf{s}_i - \mathbf{m}) \quad (15)$$

where \mathbf{C} is the covariance matrix. Vector \mathbf{m} and matrix \mathbf{C} are determined in the learning phase.

(iii) Classify a subwindow S_i for which d_i exceeds a threshold value \mathbf{a} as defective, else identify it as nondefective. i.e.,

$$S_i = \begin{cases} \text{defective} & \text{if } d_i > \mathbf{a} \\ \text{nondefective} & \text{otherwise} \end{cases}$$

The threshold value is determined by the formula

$$\mathbf{a} = D_m + \mathbf{h} (D_q - D_m) \quad (16)$$

D_m and D_q are, respectively, the sample median and the upper quartile of the order statistics D_i (distances d_i arranged in ascending order) and \mathbf{h} is a constant determined experimentally. So, the second term of

summation in Eq. (16) is the confidence interval. For an 256x256 sized image partitioned into subwindows of size 32x32, $D_m = (D_{32} + D_{33}) / 2$ and $D_q = (D_{48} + D_{49}) / 2$.

Intuitively, what the classifier does is to assign as defective the image parts (subwindows) with considerable difference from the rest. In calculating the threshold, for an image, the median of the distances of subwindows from the learned sample in place of mean is used. This is important, because if there are defective subwindows, the mean will not be a reliable measure.

IV. IMPLEMENTATION AND RESULTS

One possible application domain for the texture defect detection algorithms, among many others, is the textile fabric inspection. Hence, for the experimental justification of the algorithm, real fabric images acquired by a CCD camera in a laboratory environment are used [7]. The database consists of 36 256x256 sized 8-bit long gray level images. Seventeen of those images are void of defects while each of the remaining 19 contains defects of different size (extended-localized) and nature (point-line) that occur most frequently in the production process (Fig.2). Training of the system is attained by 16 defect free images. The rest of the set has been used for testing the algorithm. Decomposition of raw images into subbands is performed using Battle-Lemarie wavelet filter coefficients. Before computing the co-occurrence matrices, subband images are quantized into 8 levels. This results in enormous computational saving while extracting the (ENT, CON, ASM and IDM) features, without any significant effect on the final results. Window size used in scanning the image depends both on the resolution of the camera used for image acquisition and the textural properties of the fabrics. In the experiments, the highest performance (90.78%) is obtained by using 32x32 sized non-overlapping windows for the original image. This performance can be slightly improved, at the expense of the computation time, by introducing some sort of overlap between the subwindows for better treatment of thin line defects occurring at the border of the adjacent cells. In the experiments, the value of constant C in step (v) of the feature extraction algorithm is chosen as 0.35. For this value, only the LL band is retained. For comparison purposes, the MRF based method [3] and the SDCM method, with the same features that are used

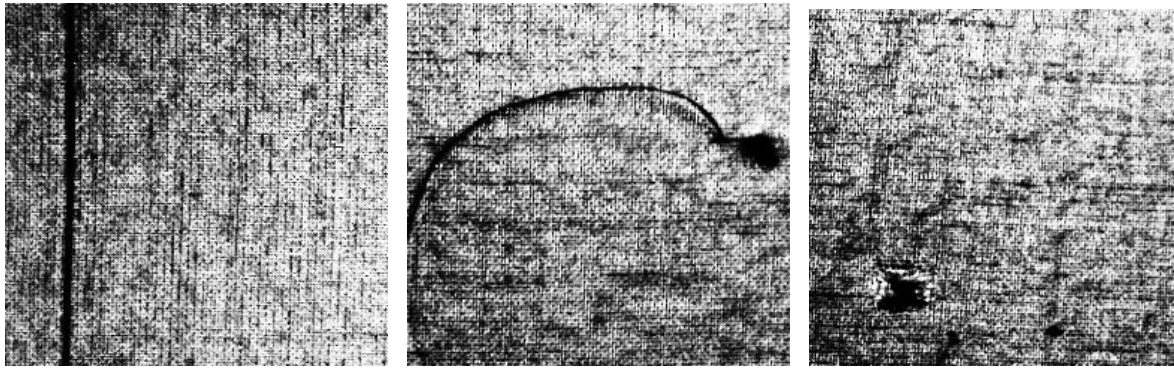


Fig.3 Examples of defective textile fabric images

in SBCM method, are implemented for the available database. In Fig.4, the correct detection versus false alarm rates, known as receiver operating curve for the three methods are plotted. The classification rates for the three set of features are depicted in Fig.5. The classification rate, CR, is defined as:

$$CR=100 * (N_{cc} + N_{dd}) / N_{total} \quad (17)$$

where N_{cc} , N_{dd} and N_{total} are, respectively, the number of subwindows being classified as clean when they are clean, the number of subwindows being classified as defective when they are defective and the total number of subwindows being tested. Results, as depicted in Figs.4-5, demonstrate clearly the advantage of the proposed algorithm that incorporates some sort of frequency information on the features by the use of subband decomposition scheme. In order to show the power of SBCM features over the SDCM, the distance values of the subwindows for the defective fabric "dc17"(Fig.6) are plotted in Fig.7. It is very interesting to notice how the defective cells have been enhanced with respect to the clean ones in the SBCM method [7].

V. CONCLUSIONS

In this paper, a new texture defect detection method based on SBCM features is introduced. This, at first site appears to be strange when compared with the performance of the SDCM. One expects decrease in performance, since features are derived from lower resolution images. But if textures with frequency content mostly concentrated on a single band are considered, focusing on that particular band and discarding the others, which carry information with low discriminatory power, improves the detection performance. Comparing the proposed method with MRF [3], it is observed that performance-wise they are almost at the same level while the computational saving introduced by SBCM method is around 43% (Fig.4-5 and Table I).

REFERENCES

- [1] A.C. Bovik, M.Clark and W.S. Geisler, "Multichannel Texture Analysis Using Localized Spatial Filter", *IEEE Trans. on PAMI*, Vol. 12, pp. 55-73, Jan. 1990.
- [2] T. Chang and C.-C.Jay Kuo, "Texture Analysis and Classification with Tree-Structured Wavelet Transform", *IEEE Trans. on IP*, Vol. 2, pp. 429-441, 1993.
- [3] F.S. Cohen, Z. Fan, and S. Attali, "Automated Inspection of Textile Fabrics Using Textural Models", *IEEE Trans. on PAMI*, Vol. 13, pp. 803-808, 1991.
- [4] I. Daubechies, "Orthonormal Bases of Compactly Supported Wavelets", *Comm. on Pure and App. Mathematics*, Vol. 41, pp. 909-996, Nov. 1988.
- [5] R.M. Haralick, K. Shanmugan and Its'Hak Dinstein, "Textural Features for Image Classification", *IEEE Trans. on SMC*, Vol.3, pp.610-621, Nov. 1973.
- [6] A. Laine and J. Fan, "Texture Classification by Wavelet Packet Signatures", *IEEE Trans. on PAMI*, Vol. 15, pp. 1186-1191, Nov. 1993.
- [7] A. Latif Amet, "Texture Defect Detection Using Wavelet Transforms", M.S. Thesis, Bogaziçi University, Istanbul, Turkey, 1997.
- [8] C.S Lee, C.-H. Choi, J.Y. Choi, Y.K. Kim and S.H. Choi, "Feature Extraction Algorithm Based on Adaptive Wavelet Packet for Surface Defect Classification", *IEEE Int. Conf. on Image Proc.*, Lausanne, Sept.1996, pp. 673-675.
- [9] S. G. Mallat, "A Theory for Multiresolution Signal Decomposition: The Wavelet Representation", *IEEE Trans. on PAMI*, Vol.11, pp. 674-693, July 1989.
- [10] P.P.Ohanian and R.C.Dubes, "Performance Evaluation for Four Classes of Textural Features", *Pattern Recognition*, Vol. 25, pp. 819-833, Aug. 1992.

[11] L.H. Siew, R.M. Hodgson and E.J. Wood, "Texture Measures for Carpet Wear Assessment", *IEEE Trans. on PAMI*, Vol. 10, Jan. 1988.

[12] J.S. Weszka, C.R. Dyer and A.Rosenfeld, "A Comparative Study of Texture Measures for Terrain Classification", *IEEE Trans. on SMC*, Vol.6, pp.269-285, 1976.

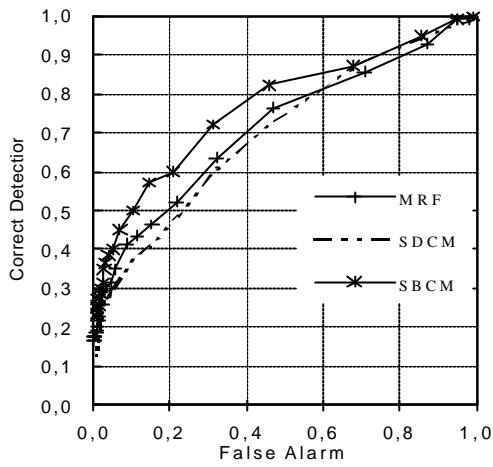


Fig.4 System Operating Curve

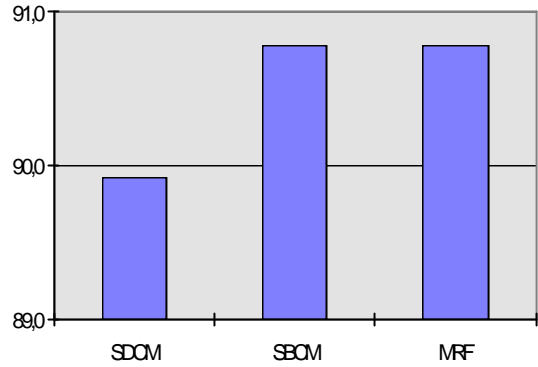


Fig.5. Classification Rates (%)

Table I. Computational Complexities

METHOD	ADDITIONS ($\times 10^6$)	MULTIPLICATIONS ($\times 10^6$)
SDCM	0,46	0,18
SBCM	0,96	0,92
MRF	1,64	1,64

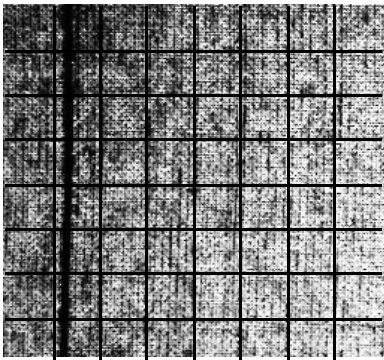


Fig.6. Defective fabric image "dc17" partitioned into 32x32 subwindows (S_i : $i=1$ to 64).

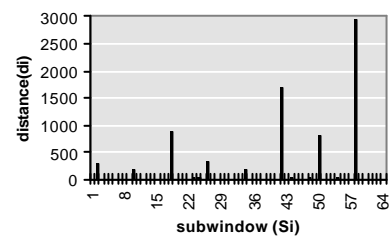
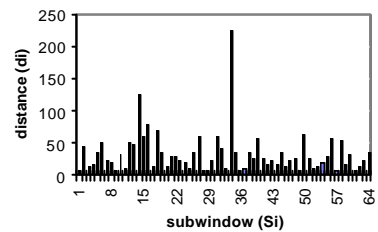


Fig.7. Distance (d_i) values for the subwindows (S_i) of defective image "dc17" obtained using SDCM (top) and SBCM (bottom).